EVALUATION ON IN-VESSEL MELT RETENTION FOR VVER1000 REACTOR UNDER SBO ACCIDENT

DOAN Manh Long(1), **TRAN Chi Thanh**(1), **NGUYEN Van Thai**(2)
(1) Viet Nam Atomic Energy Institute, 59 Ly Thuong Kiet, Hoan Kiem, Ha Noi, Viet Nam
(2) Ha Noi University of Science and Technology, 01 Dai Co Viet, Hai Ba Trung, Ha Noi, Viet Nam
Email: longdoanmanh28@gmail.com; tranchithanh@vinatom.gov.vn;
thai.nguyenvan@hust.edu.vn

ABSTRACT

In this paper, a new analytical method is developed from original In-Vessel Melt Retention with the aim of predicting heat load from a two-layer stratified molten pool to VVER1000 lower head wall under Station Black-Out (SBO) accident accompanied with reactor vessel external cooling strategy. The MELCOR code is used to study the accident consequence in order to provide initial conditions for calculation of the new method. The results show that heat load imposed from the metallic layer exceeded critical heat fluxes of external reactor vessel cooling water.

KEY WORDS
In-Vessel Melt Retention, VVER1000, MELCOR, SBO, Severe accident

1. INTRODUCTION

In case of core melt accident, it will lead to establish a molten corium pool in lower plenum if there are not any measures to suspend core degradation and prevent relocation of core debris to lower plenum. A molten corium pool in lower plenum threatens the integrity of reactor vessel, and raises concern of radioactivity release. For the first time, a novel strategy [**1**] has been proposed with the aim of confining molten pool in reactor vessel, through submerging reactor vessel in water and sufficiently cooling down molten corium pool through external reactor vessel, known as In-Vessel Melt Retention (IVR).

The IVR strategy has been, so far, successfully adopted as severe accident management strategy for low power reactors, namely AP600 [**1**] and VVER440 reactor [**2**]. Recently, it has been introduced for advanced passive high power reactors such as AP1000 [**3**] and APR1400 [**4**]. However, these studies also pointed out that, compared to low power reactors, IVR application for high power reactor was a challenging issue because of higher decay heat power and complicated accident consequence.

A value used to evaluate success of the IVR strategy is known as the safety margin. The safety margin is defined by ratio between critical heat flux (CHF), known as capability of externally cooling ambient, and heat load cause by molten pool along lower head vessel curvature. For heat load evaluation, along with experimental studies, there have been many efforts dedicated to develop theoretical methods, such as analytical method [**1**], numerical methods [**5-7**], and lump parameter method integrated in severe accident codes [**8-9**]. The analytical method [**1**], compared to other methods in term of engineering, is simpler and only calculated for simple 2-demension molten pool configuration. However, it could provide good results and its calculation is simple, less time consumption and less expensive.

Recently, the IVR concept has been introduced for higher power VVER reactors namely VVER600 [**10**] and VVER1000 [**11-14**]. The IVR studies for VVER1000 have been done by using ASTEC showed that there was not failure of lower head vessel in both Large Break Loss of Coolant accident [**11, 12**] and Station Black-Out [**13**]. In the contrary, the results in [14] by using MELCOR code presented that there was a failure of lower head vessel in case of LBLOCA plus SBO. Therefore, before proving final judgment on possibility of IVR application for VVER1000, it is necessary to take more studies on IVR strategy for VVER1000.

The paper presents an analytical method derived from original analytical IVR method proposed by Theofanous et al., [**1**]. The new method is, referred as Modified-IVR (MIVR), used to evaluate heat load along VVER1000 lower head curvature imposed by a two-layer stratified molten pool in case of SBO accident. The MELCOR code was used to analyze in-vessel accident consequences from initiation of accident to the failure of lower core support plate. The purpose of MELCOR calculation is to determine the configuration of two-layer stratified molten pool formed in VVER1000 lower plenum. The results obtained by MIVR method indicated that the heat flux distribution on external surface of lower head wall exceeded the critical heat fluxes at locations contacting to metallic layer.

2. MELCOR INPUT MODEL FOR VVER1000

MELCOR code [**8**] is an integrated severe accident code, which has been developed by Sandia Laboratory. MELCOR code can simulate wide range of accidents with a series of consequential phenomena in light water reactors. Therefore, it will be a good assistant for stand-alone analytical method in this case.

The VVER1000 reactor is a Russian pressurized water reactor, which consists of four primary circulation loops, with 3000 MW thermal power and 1000 MW electric power. Each closure loop comprises a main coolant pump and a horizontal steam generator. The reactor core consists of 163 fuel assemblies (FAs) and each FA comprises 312 fuel rods; 61 FAs additionally contain 18 control rods per assembly.

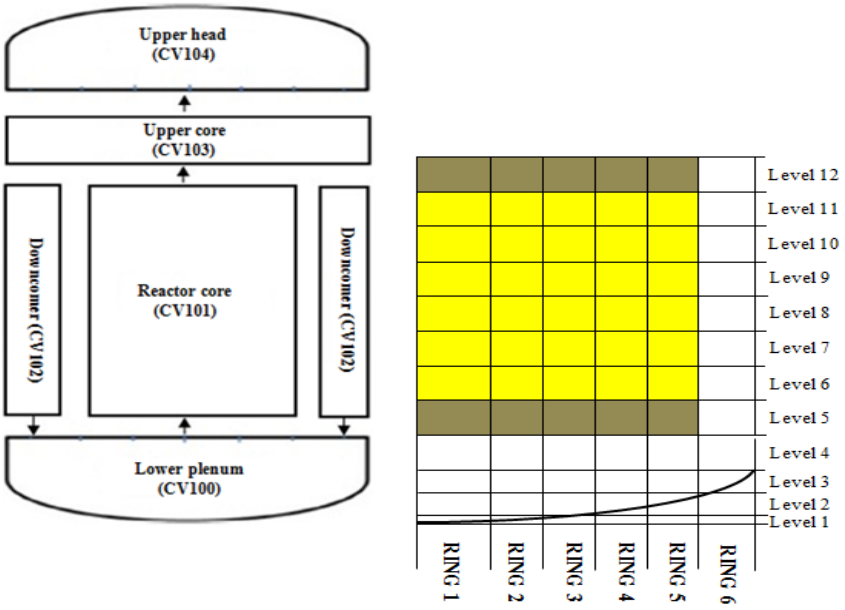

Figure 1: Nodalization of thermal hydraulics volume (left) and structure inside reactor vessel (right)

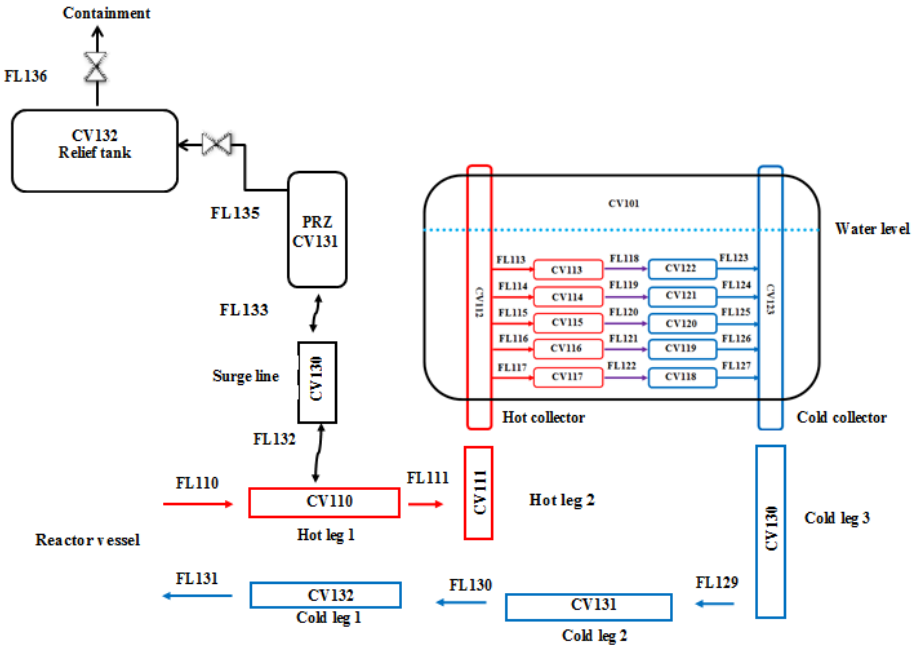

Figure 2: Nodalization of loop 1 including primary and secondary part

Thermal hydraulics volume of reactor vessel comprises of lower plenum, reactor core, down-comer, upper plenum, upper head which are assigned as following identifiers CV100, CV101, CV102, CV103 and CV104 respectively (Fig.1). Radically, the reactor core and lower plenum are divided into 5 concentric rings and 6th is for downcomer (Fig.1). In axial direction, the lower plenum is subdivided into 4 levels, the 5th presents for lower core support plate, the reactor core is represented from 6th to 11th level, and the 12th level represents for upper core support plate.

The four circulation loops are modeled separately but have the same scheme. Figure 2 demonstrates nodalization scheme of the first loop including the pressurizer: hot leg is represented by two control volumes (CV110 and CV111) and cold leg is divided into three control volumes (CV130, CV131 and CV132); heat exchanger tubes in steam generator are separated to five stages and each stage is split into two parts such as hot part with red boundary and cold part with blue boundary; hot collector and cold collector are modeled as control volumes (CV112 and CV123); pressurizer systems comprises of surge line, pressurizer and relief tank, are also modeled. The secondary part in steam generator is modeled as a single control volume (CV101);

3. MIVR and verification calculations

3.1. The model of MIVR

The MIVR is developed from the original IVR model proposed by Theofanous et al., [**1**]. The original model was applied to evaluate heat load from a two-layer molten pool to hemispherical-shaped lower head vessel likely AP600 reactor (Fig.5). In this model, the molten pool completely located in hemispherical lower plenum and heat flow in oxidic pool comprised of two elements, namely downward and upward (Fig.5). However, for VVER reactors, the semi-elliptical part of lower head vessel could not cope with the volume of oxidic pool in case of relocation of total core structure to lower plenum, therefore, part of oxidic pool will occupy the

volume of cylindrical part of lower head vessel. Hence, in order to apply the original IVR model for VVER reactors, it is necessary to add a component representing for heat flow transferring to the cylindrical part of VVER lower head vessel into energy balance equation of oxidic pool.

Therefore, the MIVR model is only different to the original model by an additional component in the energy balance equation of oxidic pool. Then, the energy partition in oxidic pool of MIVR is split into three components (upward, downward and sideward) instead of two components (upward and downward) as in original model. The downward flow represents heat flow to elliptical curvature, the sideward flow represents to cylindrical part, and the last one is respect to heat flow transferring to above metallic layer (figure 6). Additionally, the radiation heat flows from other components to molten pool are ignored in MIVR. Then, the MIVR model is described as following.

Energy partition in oxidic pool:

$$\dot{Q}V = q_{up}S_{up} + q_{dn}S_{dn} + q_{sd}S_{sd} \quad (1)$$

$$q_{up} = \frac{QV}{(R1\,S_{up} + S_{dn})} \quad (2)$$

$$q_{sd} = \frac{QV}{(R2S_{up} + S_{dn})} \quad (3)$$

$$q_{dn} = \frac{QV - (q_{dn}S_{dn} + q_{sd}S_{sd})}{S_{up}} \quad (4)$$

$$R1 = \frac{Nu_{up}}{Nu_{dn}} = \frac{q_{up}}{q_{dn}} \quad (5)$$

$$R2 = \frac{Nu_{sd}}{Nu_{dn}} = \frac{q_{sd}}{q_{dn}} \quad (6)$$

$$\frac{q_{dn}(\theta)}{q_{dn}} = f\left(\frac{\theta}{\theta_p}\right) \quad (7)$$

$$q_{dn}(\theta) + \frac{Q\,\delta 1_{cr}}{2} = \frac{k_{cr}}{\delta 1_{cr}}(T_m - T_w) \quad (8)$$

$$\frac{k_{cr}}{\delta 1_{cr}}(T_m - T_w) = \frac{k_w}{\delta 1_w}(T_w - T^{**}) \quad (9)$$

$$q_{sd} + \frac{Q\,\delta 2_{cr}}{2} = \frac{k_{cr}}{\delta 2_{cr}}(T_m - T_w) \quad (10)$$

$$\frac{k_{cr}}{\delta 2_{cr}}(T_m - T_w) = \frac{k_w}{\delta 2_w}(T_w - T^{**}) \quad (11)$$

These equations (8), (9), (10) and (11) are iteratively solved to get the values of corium crust thickness, reactor vessel thickness and then the heat flux to water of external surface of lower head vessel would be obtained.

Light metallic layer:

$$q_{l,i} = q_{up} + \frac{Q\,\delta_{cr,top}}{2} = \frac{k_{cr}}{\delta_{cr,top}}(T_m - T_{l,i}) \quad (12)$$

$$q_{l,i} = h_b(T_{l,i} - T_b) \quad (13)$$

$$q_{l,i}S_{l,i} = q_{l,w}S_{l,w} + q_{l,o}S_{l,o} \quad (14)$$

$$q_{l,o} = h_{l,t}(T_b - T_{l,o}) = \epsilon\sigma T_{l,o}^4 \quad (15)$$

$$q_{l,w} = h_{l,w}(T_b - T_{l,m}) = \frac{k_w}{\delta_{l,w}}(T_{l,m} - T^{**}) \quad (16)$$

The equations (12) and (13) are also iteratively solved to obtain heat flux transferring to upper metallic layer, crust thickness between oxidic pool and metallic layer, and temperature of bottom surface of metallic layer. Then, the system of equations (14), (15), and (16) are solved iteratively, after adapting values obtained from solution of equations (12) and (13), to get upward heat flux, sideward heat flux and lower head vessel thickness.

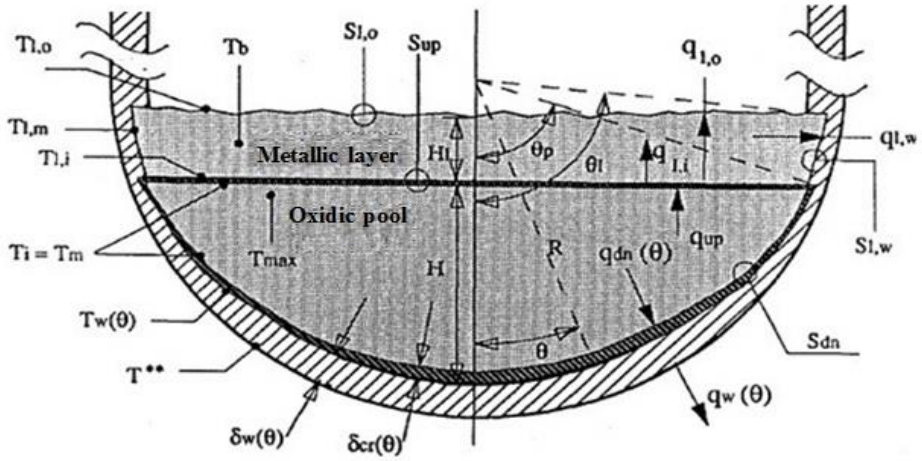

Figure 5: Energy partition of the two-layer stratified motel pool in hemispherical shape [1]

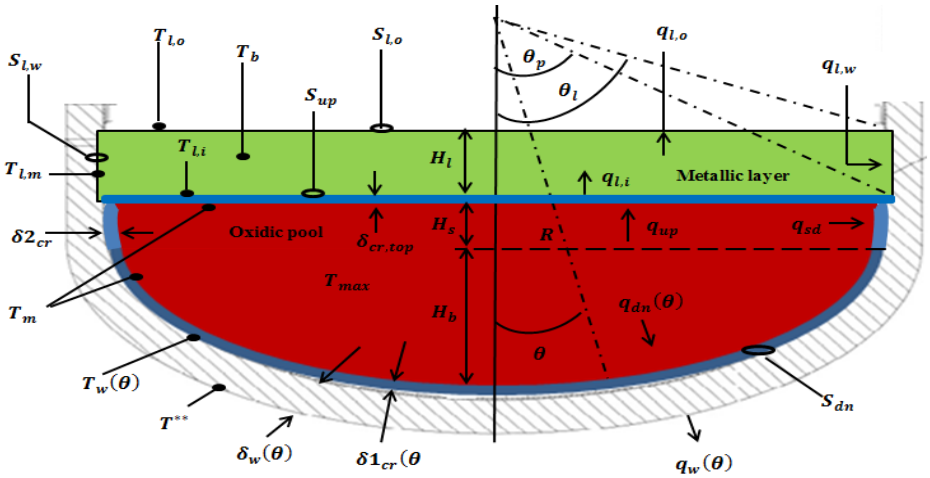

Figure 6: Energy partition of two-layer stratified molten pool in semi-elliptical shape

Finally, it is assumed that the heat transfer regime from lower head wall to water in cooling channel is nucleate boiling regime. The heat transfer coefficient is Rohsenow's correlations [**3**].

3.2. Verification of MIVR

3.2.1. Benchmark calculation for AP600

In this section, MIVR model is verified by benchmark calculation based UCSB-assumed final boundary state for two-layer stratified molten pool [**1**] and ERI input description [**3**]. In this calculation, the molten pool entirely locates in hemispherical lower plenum (Fig.5), therefore, the sideward heat flow will not be taken account in MIVR model. The results obtained from MIVR are heat flux transferring to water, corium crust thickness and vessel wall thickness, which would

be compared to UCSB results and INEEL results given in [**3**]. The heat transfer correlations in oxidic pool and metallic layer for MIVR, UCSB and INEEL calculations are presented in table 1.

Table 1: Heat transfer correlation in models

Pool/layer	Metallic layer	Oxidic pool
UCSB	**Top and bottom surface** *(Globe-Dropkin "Specialized"):* $Nu = 0.15Ra^{1/3}$ **Side wall** *(Churchill-Chu):* $Nu_{sd} = 0.076Ra^{1/3}$	**Top surface** *(Mini-ACOPO):* $Nu_{up} = 0.345Ra^{0.233}$ **Bottom surface** *(Mini-ACOPO):* $Nu_{dn} = 0.0038Ra^{0.35}\left(\frac{H}{R}\right)^{0.25}$
INEEL	**Top and bottom surface** *(Globe-Dropkin):* $Nu_{up} = 0.069Ra^{0.333}Pr^{0.074}$ **Side wall** *(Churchill-Chu):* $Nu_{sd} = \left[0.825 + \left(\frac{0.387Ra^{1/6}}{[1+(0.492/Pr)^{9/16}]}\right)\right]^2$	**Top surface** *(ACOPO):* $Nu_{up} = 2.4415Ra^{0.1772}$ **Bottom surface** *(ACOPO):* $Nu_{dn} = 0.1857Ra^{0.2304}\left(\frac{H}{R}\right)^{0.25}$
MIVR	**Top and bottom surface** *(Globe-Dropkin "Specialized"):* $Nu = 0.15Ra^{1/3}$ **Side wall** *(Churchill-Chu):* $Nu_{sd} = 0.076Ra^{1/3}$	**Top surface** *(Mini-ACOPO):* $Nu_{up} = 0.345Ra^{0.233}$ **Bottom surface** *(Mini-ACOPO):* $Nu_{dn} = 0.0038Ra^{0.35}\left(\frac{H}{R}\right)^{0.25}$ **Side wall** *(Steinberner and Reineke, 1978)* $Nu_{sd} = 0.85Ra^{0.19}$

As seen in figure7, heat flux predicted from MIVR, UCSB and INEEL calculation are quite different at lowest locations of oxidic pool (between 0 – 35^o) and slightly different in the rest of oxidic pool. The heat flux peak at transition between oxidic pool and metallic layer predicted by UCSB is highest, whereas this value predicted by MIVR and INEEL was almost similar. For locations adjacent to metallic layer, MIVR heat flux is highest, and INEEL prediction is lowest. The remain reactor vessel wall thickness obtained from calculation is presented in figure 8 which showed wall thickness bounding oxidic pool predicted by MIVR is smallest and INEEL prediction is larger than UCSB. However, there is significant change in vessel bounding metallic layer, IVMR prediction is highest and INEEL value is smallest. Figure 9 shows corium thickness obtained from calculations. At locations between 0 to 50^o, USCB calculation is smallest and MIVR calculation is largest. At the rest locations, calculations are quite similar.

The differences in these calculations may be accounted for the difference in heat transfer correlations for molten pool, conductivity of corium thickness and vessel wall, and other input parameters. Comparison results as showed in figures 7, 8 and 9 proves that MIVR correctly interpreted equations in UCSB analysis.

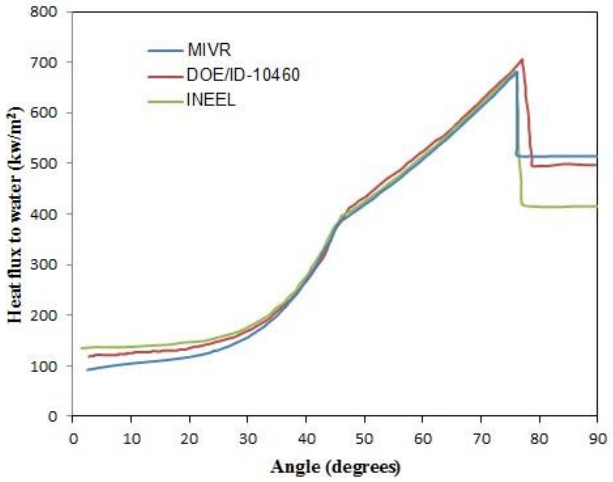

Figure 7: Comparison of MIVR heat flux with UCSB and INEEL heat fluxes

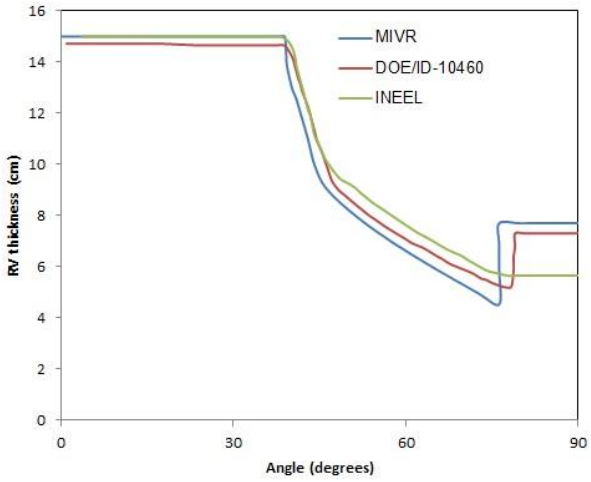

Figure 8: UCSB, INEEL and MIVR predictions for LH vessel thickness

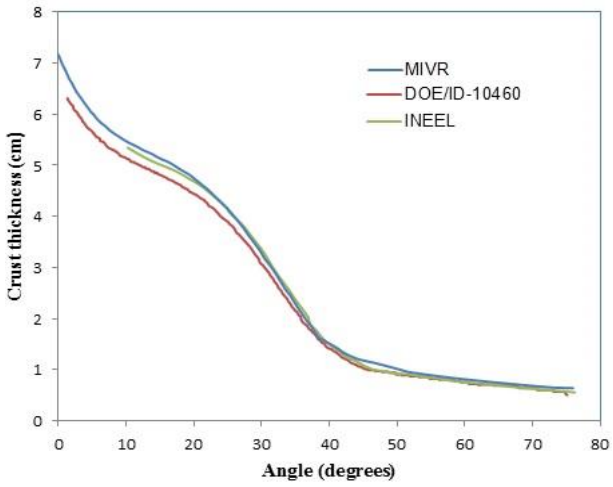

Figure 9: UCSB, INEEL and MIVR predictions for corium crust thickness

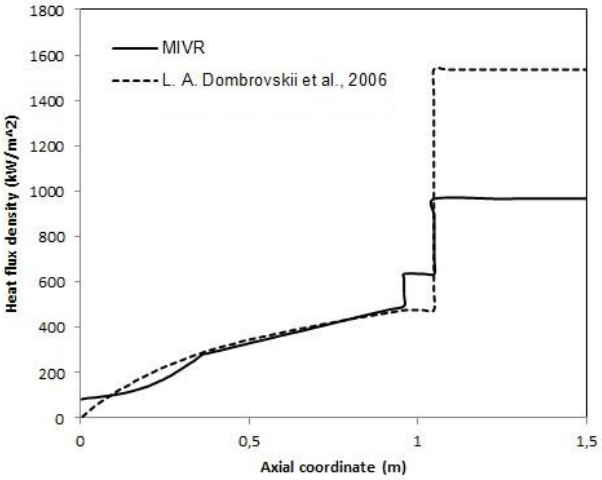

Figure 10: Heat flux density to the VVER440 lower head wall

3.2.2. Calculation for VVER440

In this part, the MIVR is applied to predict to heat load to VVER440 lower heat vessel by final boundary state of molten pool configuration with case designated as case 1 presented in [**15**]. The basic input parameters of the molten pool are $H_b = 0.96\ m$, $H_s = 0.09\ m$, $H_l = 0.455\ m$, heat flux density $\dot{Q} = 1.5\ MW/m^3$, emissivity $\epsilon = 0.4$, initial vessel wall $\delta = 0.14\ m$, liquidus temperature of oxidic pool $T^m = 2700K$ and liquidus temperature of metallic layer $T_{l,m} = 2700K$. Dombrovskii et al. [**15**] used a combined model, which originated from numerical model and heat balance model to predict density of heat flux to vessel wall. The heat load in axial direction of molten pool predicted by MIVR is compared to that of case 1 in [**15**] showed in figure 10.

The result showed that the heat densities to vessel wall along with axial coordinate of molten pool predicted by MIVR at lowest position between 0 to 0.3 m are different to results predicted by Dombrovskii et al.[**15**]. In range of height between 0.3 m to 0.95 m, MIVR results are similar to predictions in [**15**]. In the cylindrical part of oxidic pool with the range from 0.96 m to 1.05 m, MIVR calculation showed that the predicted heat load is higher than that of Dombrovskii et al.[**15**]. A heat flux peak also was observed at the transition point between oxidic

pool and metallic layer. However, heat load from metallic layer predicted by MIVR is much smaller than that of Dombrovskii et al.[**15**], the peaks are 967 kW/m^2 and 1540 kW/m^2 respectively. In general, heat flux densities imposed from oxidic pool predicted by MIVR were higher than that of Dombrovskii et al.[**15**]. This finding partly explained the reason of smaller heat flux from metallic layer in MIVR was smaller than prediction in [**15**] in range of height between 1.05 m to 1.5 m, and the other reasons might come from differences in initial conditions.

The value of increase of heat density to vessel wall at transition point is increased and the average heat flux on the vertical cylinder is uniform as seen in results obtained from COPO I&II experiments [**16**]. Therefore, MIVR has shown the capability of evaluating the heat density imposing on internal surface of lower head vessel shape like VVER reactors from molten pool.

4. DEFINITION OF ACCIDENT SCENARIO

The hypothetical severe accident studied in this paper is the SBO accident accompanied with externally vessel cooling. Following is the main assumption of the scenario:

- Loss of offsite and onsite power including diesel generator and batteries except batteries for BRU-A valves of SGs;
- Loss of all active safety systems;
- Failure of Emergency Feed Water;
- Pressure of PRZ was controlled by relief valves and safety valves with characteristics in table 2;
- There was not taken into account main coolant pumps seal leakages;
- Pressure of SGs is control by BRU-A valves to maintain pressure in SGs below 6.7MPa;
- Four hydro-accumulator are available;
- The depressurization for reactor vessel by opening safety valves on top of PRZ and cavity flooding strategy will be triggered when temperature of steam in reactor core exceeds 650^{o}C;
- With the aim of providing initial parameters for MIVR, MELCOR simulation is stopped at 15000 seconds since begin of accident.

Table 2: Pressurizer safety valve characteristics

Name	Characteristics	Design value	MELCOR value
Relief valves	Opening pressure (MPa)	16.0	16.0
	Closing pressure (MPa)	15.7	15.7
Safety valves Stage 1	Opening pressure (MPa)	18.11	18.11
	Closing pressure (MPa)	16.67	16.67
Safety valves Stage 2, 3	Opening pressure (MPa)	18.6	18.6
	Closing pressure (MPa)	17.07	17.07

5. INITIAL CONDITIONS OF ACCIDENT SCENARIO

The basic parameters obtained from MECLOR simulation for VVER1000 under steady state condition are compared to design values (table 3).

Table 3: Comparison of parameters at steady state condition

Parameteres	MELCOR value	Design value
Core power (MW)	3100	3000+210
Primary pressure (MPa)	15.6	15.7±0.3
Maximum coolant temperature at reactor intlet (^{o}K)	567	559.15±2.0
Average coolant temperature at reactor outlet (^{o}K)	596	593.15±3.5
Mass flow rate through reactor core (kg/s)	17650	17 611
Pressure in steam generator (MPa)	6.29	6.28±0.2
Steam mass flow rate at steam generator outlet (kg/s)	420	437

6. RESULTS AND DISCUSSION

6.1. Accident progression from MELCOR simulation

MELCOR code is aimed at providing initial conditions for MIVR calculation. MELCOR calculation is stopped at 15000 seconds since begin of accident. The main events of the scenario are given in table 4.

Table 4: The timing of main events

Main events	TIME (second)
Accident happened	0.0
Reactor tripped	1.6
Temperature of steam in core exceeded 650^{o}C	9723.7
Start of HAs injection	9906.6
Start of fuel cladding rupture	10300.0
Massive relocation of core debris to lower plenum Due to failure of lower core support plate	11550.0
Lower plenum totally dried out	11600.0
Stop of HAs injection	13000.0
Reactor core totally dried out	13050.0
Stop calculation	15000.0

The reactor is tripped after 1.6 seconds since start of the accident. The sudden drop of pressure in primary loops (figure 11) is a result of reactor shutdown, which reduces reactor power to decay heat power. Since decay heat continuously heats reactor core which leads to increase of pressure in primary loop. The fluctuation of pressure (figure 11) in primary loop is due to open and close of relief valves and safety valves when it reaches to these set points. At 9723.7 seconds, temperature of steam in reactor core is observed to exceed 650^{0}C, which triggers the opening of safety valves to depressurize for reactor vessel. The depressurization causes the sharp descend of pressure in primary loop (figure 11).

Before the occurrence of depressurization, water in reactor vessel totally evaporates (figure 12). When the depressurization is initiated, pressure in reactor vessel quickly decreased to below set points of HAs (figure 11) at 9906.6 seconds. Additional water from four hydro accumulators (HAs) is partly recovered reactor core (figure 12). However, the additional water from HAs was not enough to sustain the re-flooding and the reactor vessel secondly losses water completely at 13000s (figure 12).

The oxidation reactions happen at 10000 seconds and the total mass of hydro generated is nearly 400 kg (figure 13). When re-flooding do not last long enough together with the exo-

thermal oxidation reactions causes collapse of fuel cladding at 10300s at central of reactor core (figure 14). Figure 14 demonstrates cladding temperature of core ring 1, the temperature lines go down to zero means that the cladding structures are collapsed. Following degradation of core structure, lower core support plate is observed to be failed at 11500s triggering massive relocation of core debris to lower plenum. Total mass of core debris in lower plenum predicted by MELCOR is given in Table 5.

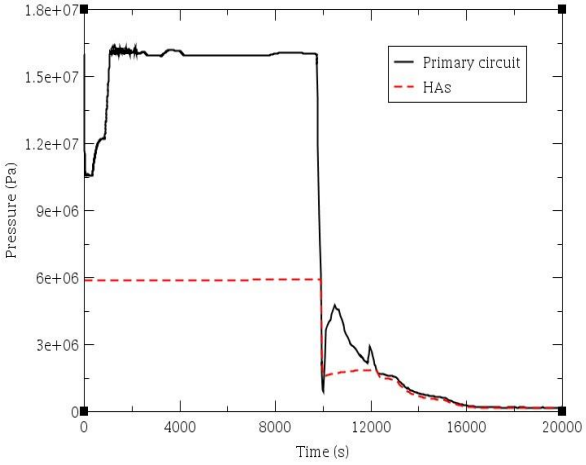

Figure 11: Pressure in primary circuit (solid line) and in HAs (dash line)

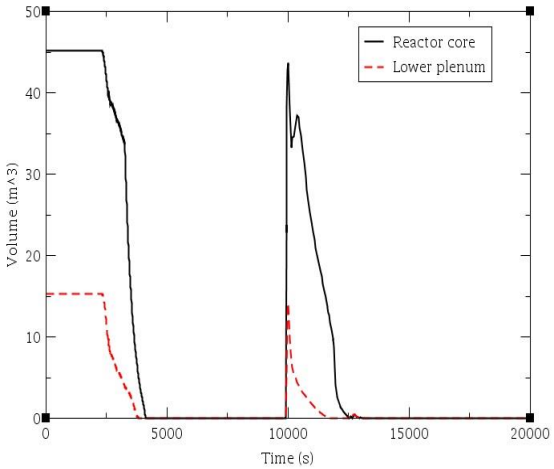

Figure 12: Collapsed volume of water in reactor core (solid line) and lower plenum (dash line)

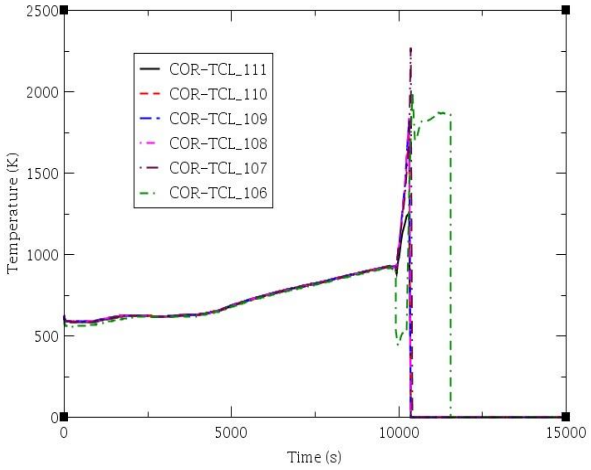

Figure 13: Temperature of cladding in ring 1

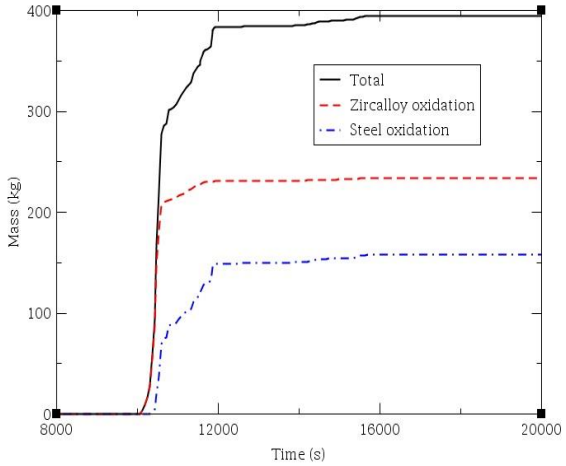

Figure 14: Mass of hydrogen generated in reactor vessel

Table 5: Mass of debris in lower plenum

Components	Mass (kg)
UO2	80600
Zr	19370
ZrO2	7150
Steel	29260
Oxide of steel	5200

6.2. Results from MIVR calculation

6.2.1. Define initial and boundary conditions

MELCOR calculation shows that lower core support plate failed at 11500s and total components mass of debris bed is presented in table 5. Temperature of debris in lower plenum at 11500s is assumed at 500 K uniformly and components of debris bed are grouped in two groups as oxide debris (UO2+ZrO2+oxide steel) and metallic debris (steel+Zr). The thermal characteristics of debris bed are listed in table 6.

Table 6: Thermo-physical properties of debris [10]

Property	Oxide debris	Metal debris
λ, (W/m.K)	4.0	20.0
C_p, (J/kg.K)	561	654
ρ, (kg/m^3)	7560	6500
T_{liq}, (K)	2700	1750
L (MJ/kg)	0.247	0.279
β, (1/K)	1.0x10^{-4}	1.5x10^{-4}
μ, (Pa.s)	3.4x10^{-3}	3.06x10^{-4}

The need energy is to liquate oxide debris and metal debris is given below:

$$Q = m \times \{C_p \times (T_{liq} - T_{ini}) + L\} \quad (17)$$

From equation (17) and thermo-physical properties of debris, the need energy to liquate oxide debris and metal debris are 137.68 GJ and 53.32 GJ respectively, total is 191 GJ. Because all UO2 in reactor core relocated to lower plenum, so the decay heat released in debris bed is based on core decay heat power from MELCOR calculation (figure 15). A fit function is used to roughly estimate amount of time when the debris bed is melt into liquid. The fit function is given following:

$$P = 471.76 \times t^{-0.3} \quad (18)$$

Form equations (17-18), the amount of time is to liquate debris bed since 11500 seconds is estimated by solving the following equation:

$$\int_{11500}^{t} 471.76\, t^{-0,3} = 191000 \quad (19)$$

By solving equation (19) with taking account of 20% decay lost from volatile product, the time which debris bed is completely melt at 20700s since accident happened. The decay heat at 20700s is 19.14 MeV and assumed to be generated only in oxidic pool.

The volume of oxidic pool is 12.3 m^3, whereas volume of semi-ellipsoid head of VVER1000 reactor vessel is about 7 m^3 and height (H_b) of 0.965 m. The oxidic pool, therefore, completely occupied volume of semi-ellipsoid head and the remaining volume contacted to cylindrical part of lower head vessel with the height (H_s) of 0.392 m. The volume of metallic layer was 7.5 m^3, and totally located in cylindrical part of reactor vessel with the height (H_l) of 0.56 m. The configuration of molten pool in VVER1000 lower plenum and nomenclature of physical parameters are demonstrated in figure 6, and the heat transfer correlations for oxidic pool and metallic layer were presented in table 1. The emissivity of metallic layer is taken as 0.45.

6.2.2. Calculation results

The thermal distribution along external VVER1000 lower head vessel predicted by MIVR is presented in figure 16. The results show that there is intensive heat load from metallic layer to lower head wall from axial height of 1.33 m to 1.89 m. The intensive heat peak is predicted as 1.14 MW/m^2. The boundary effect is also observed in oxidic pool at the height of 0.965 m, in which the oxidic pool boundary changes from elliptic curve to vertical line. At the transition point, there is an increase change of heat flux trend.

In order to evaluate possibility of IVR strategy for VVER1000 in viewpoint of thermal load, the critical heat fluxes obtained from experiments on large-scale models of the VVER vessel [**17**] and from the external cooling of the vessel with boiling of water in a large volume [**18**], CHF1 and CHF2 respectively, are also presented in figure 16. The comparison between external heat flux and the critical heat fluxes shows that the head load imposed to elliptical part of lower head is well below CHF1 and CHF2 curve, whereas the heat load imposed to cylindrical part of reactor vessel by metallic layer is far larger than CHF2, and slightly smaller than CHF1.

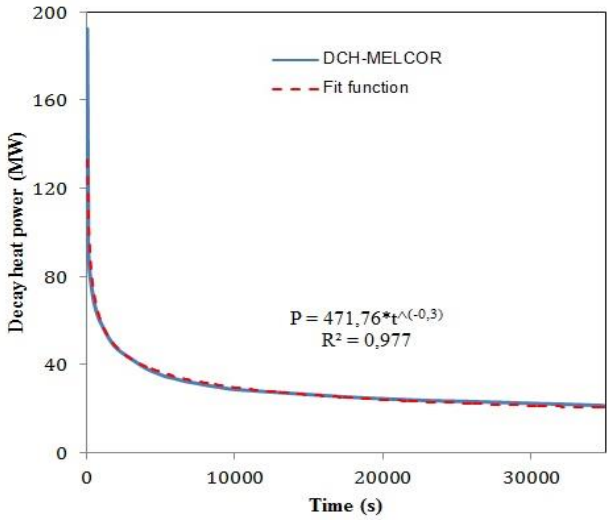

Figure 15: Decay heat released in debris bed and fit function

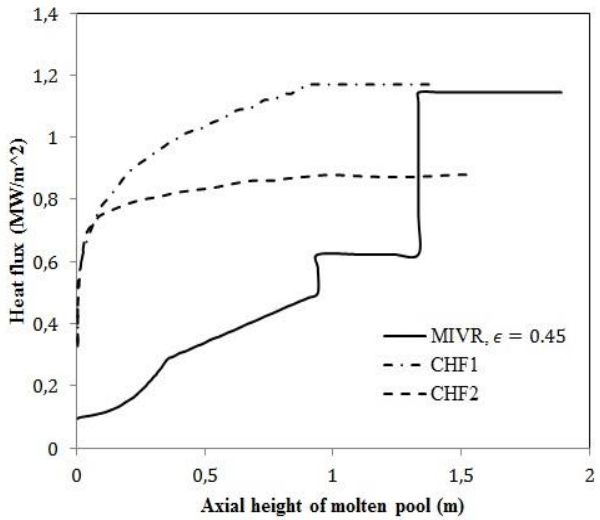

Figure 16: Heat flux to water

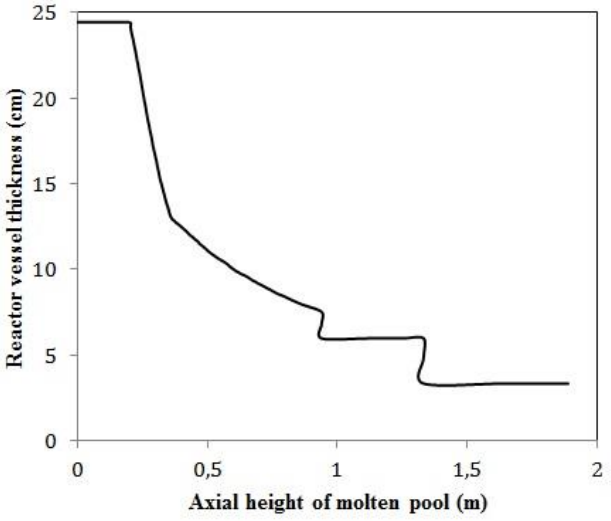

Figure 17: Reactor vessel thickness

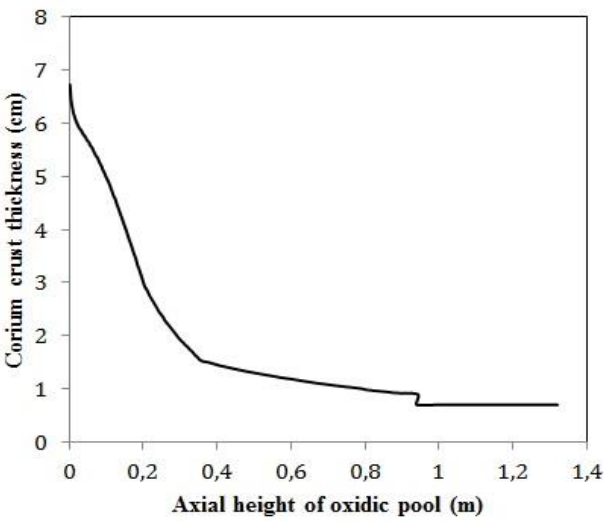

Figure 18: Corium crust thickness

The remain thickness of VVER1000 lower head wall and corium crust thickness bounding oxidic pool predicted by MIVR are presented in figure 17 and figure 18 respectively. Figure 17 shows that the smallest remain thickness of VVER1000 lower head vessel is 3,34cm at locations contacting to metallic layer. The largest corium crust thickness is predicted as 6,27cm at very bottom of oxidic pool and the smallest at locations bounding cylindrical part of oxidic pool (Fig.18).

7. CONCLUSION

In this paper, a new IVR analytical model was proposed to evaluate In-Vessel Melt Retention for VVER1000 under Station Black-Out accident accompanied by support of MELCOR code. According to obtained results, some conclusions are given following:

- A new analytical model was developed from original IVR model proposed by Theofanous et al,. [**1**], referred as Modified IVR (MIVR). The MIVR was verified through AP600 benchmark calculation and calculation for configuration of molten pool in VVER440 lower plenum [**15**]. The results showed that MIVR could be applied to predict the heat load from a two-layer stratified molten pool establishing in both hemispherical and semi-elliptical lower head vessel;
- Then, MIVR was applied to predict heat load from a two-layer stratified molten pool to VVER1000 lower head wall. The results showed that heat fluxes on external surface of VVER1000 lower wall exceeded existing critical heat fluxes in this scenario. Therefore, the IVR strategy in this scenario did not provide safety margin large enough to secure the integrity of VVER1000 reactor vessel. In the future, it is necessary to set up new experimental facilities in order to improve capability of cooling of external ambient for VVER1000 lower head vessel shaped curvature.

NOMENCLATURES

L	Latent heat
$\dot{Q}$	Volumetric heat generation heat
$q_{l,w}$	Heat flux at vessel wall in contact with metallic layer
$q_w(\theta)$	Local heat flux at vessel wall in contact with oxidic pool at angular position
q	Average heat flux at boundaries
S	Surface area
T	Temperature
T^{**}	Water saturated temperature
V	Volume of oxidic pool

Greeks

δ	Thickness
ϵ	Emissivity of metallic layer
θ	Polar angle on the lower head vessel
θ_p	Polar angle of oxidic pool top
θ_l	Polar angle of metallic layer top

Subscripts

b	Bulk value
cr	Crust value
dn	Downward
l	Metallic layer
l,i	Inner metallic boundary value
l,m	Liquidus of vessel wall in contact with metallic layer
l,o	Outer metallic layer boundary value
l,w	At vessel wal in contact with metallic layer

m Liquidus
sd Sideward
up Upward
w Vessel wall value

ACKNOWLEGEMENT
The authors are grateful for financial funding of Viet Nam Atomic Energy Institute and Ministry of Science and Technology. This work was performed under ministerial project with contract number 05/HĐ/ĐTCB signed on 05/01/2018.

REFERENCES

[1] T.G.Theofanous et al., "*In-Vessel Coolability and Retention of Core Melt*," DOE/ID-10406 Volume 1, October 1996.

[2] Kymäläinen et al., "*In-vessel retention of corium at the Loviisa plant*," Nuclear Engineering and Design, 169, 109-130, May 1996.

[3] H.Esmaili et al., "*Analysis of In-Vessel Retention and Ex-Vessel Fuel Coolant Interaction for AP1000*," NUREG/CR-6849, July 2004.

[4] J.L.Rempe et al., "*In-vessel retention of molten corium: Lesion learned and Outstanding issues*," Nuclear Technology, Vol.161, 2008.

[5] V. A. BUI and T. N. DINH, "*Modeling of Heat Transfer in Heated-Generating Liquid Pools by an Effective Diffusivity-Convectivity Approach*", *Proceedings of 2nd European Thermal-Sciences Conference*, Rome, Italy, pp.1365-1372, 1996.

[6] B. R. SEHGAL et al., "*Heat Transfer Process in Reactor Vessel Lower Plenum during A Late Phase of In-Vessel Core Melt Progression*", *J. Advances in Nuclear Science and Technology*, Plenum Publ. Corp., 1998.

[7] L.A.DOMBROVSKII et al., "*Numerical Simulation of The Stratified-Corium Temperature Field and Melting of The Reactor Vessel for A Severe Accident in A Nuclear Power Station*", *Thermal Engineering*, Volume 45, No.9, pp. 755-765, 1998.

[8] MELCOR Computer Code Manual, "*Core (COR) Package Reference Manuals*", *Version 1.8.6*, Vol. 2, September 2005.

[9] "*MAAP4 Users Manual*", *Fauske Associated Inc.*, Vol. 2, 1999.

[10] Vladimir Loktionov et al., "*Features of heat and deformation behavior of a VVER-600 reactor pressure vessel under conditions of inverse stratification of corium pool and worsened external vessel cooling during the severe accident*," Nuclear Engineering and Design 326 (2018) 320–332.

[11] Yu.A. Zvonarev et al., "*ASTEC application for in-vessel melt retention modelling in VVER plants*," Nuclear Engineering and Design 272 (2014) 224-236.

[12] P. Tusheva et al., "*Investigations on in-vessel melt retention by external cooling for a generic VVER-1000 reactor*," Annals of Nuclear Energy 75 (2015) 249-260.

[13] R. Gencheva et al., "*Study of in-vessel melt retention for VVER1000/V320 reactor*," Nuclear Engineering and Design 298 (2016) 208–217.

[14] J. Duspiva "*Analytical simulation of In-Vessel Melt Retention Strategy for VVER1000/320 reactor using MELCOR code*," Proceeding of NURETH-16, Chicago, USA, pp. 6793-6806, 2015.

[15] L. A. Dombrovskii et al.,"*Calculations of Heat Flowrates to the VVER-440 Reactor Vessel during Interaction of Corium Melt with the Reactor Vessel," Thermal Engineering*, Volume 53, No.4, pp. 302-306, 2006.

[16] Kymäläinen et al., "*Heat flux distribution from a heated volumetrically pool with high Rayleigh number*," Nuclear Engineering and Design, 149, 401-408, 1994.

[17] Yang et al., "*Correlations of Nucleate Boiling Heat Transfer And Critical Heat Flux For External Reactor Vessel Cooling*," Proceeding in ASME Summer Heat Transfer Conference, INEEL/CON-05-02604 preprint, July 17–22, 2005

[18] Zvonarev et al., "*Calculation analysis of melt active zone keeping in reactor vessel at severe accidents on NPP with VVER*," Proceeding in: Proc. 7th Int. Sci.-Tech. Conf. "Ensuring of Safety of NPP with VVER", Podolsk, OKB Gidropress, May, 2011 (in Russian).

ĐÁNH GIÁ KHẢ NĂNG GIỮ NHIÊN VẬT LIỆU NÓNG CHẢY BÊN TRONG THÙNG LÒ PHẢN ỨNG VVER1000 KHI XẢY RA SỰ CỐ SBO

Đoàn Mạnh Long[(1)], Trần Chí Thành[(2)], Nguyễn Văn Thái[(3)]

(1) Trung tâm Đào tạo hạt nhân, 140 Nguyễn Tuân, Thanh Xuân, Hà Nội
(2) Viện Năng lượng nguyên tử Việt Nam, 59 Lý Thường Kiệt, Hoàn Kiếm, Hà Nội
(3) Đại học Bách Khoa Hà Nội, 01 Đại Cồ Việt, Hai Bà Trưng, Hà Nội

Email: longdoanmanh28@gmail.com; tranchithanh@vinatom.gov.vn; thai.nguyenvan@hust.edu.vn

GIỚI THIỆU

Trong bài báo này, một phương pháp tính toán giải tích đã được phát triển từ một mô hình tính toán đánh giá khả năng giữ nhiên vật liệu nóng chảy bên trong thùng lò phản ứng ban đầu, với mục đích đánh giá tác dụng nhiệt từ một bể vật chất nóng chảy phân hai tầng (lớp kim loại ở trên và bể ôxit ở dưới) vào thành thùng lò phản ứng VVER1000, khi xảy sự cố Mất hoàn toàn nguồn điện (SBO), có áp dụng biện pháp làm mát bề mặt ngoài vỏ thùng lò phản ứng. Chương trình MELCOR được sử dụng để cung cấp các dữ kiện đầu vào cho mô hình tính toán giải tích. Kết quả tính toán cho thấy giá trị thông lượng nhiệt tác dụng vào vỏ đáy thùng lò phản ứng VVER1000 vượt quá giá trị thông lượng nhiệt tới hạn của môi trường làm mát bên ngoài tại vị trí tiếp xúc với lớp kim loại.

TỪ KHÓA
Biện pháp IVR, VVER1000, MELCOR, SBO, sự cố nghiêm trọng